行政院國家科學委員會專題研究計畫　期中進度報告

子計畫二：寬頻無線通訊之低功率基頻訊號處理(2/3)

計畫類別：整合型計畫
計畫編號：NSC93-2220-E-009-015-
執行期間：93 年 08 月 01 日至 94 年 07 月 31 日
執行單位：國立交通大學電子工程學系暨電子研究所

計畫主持人：桑梓賢
共同主持人：許騰尹

報告類型：完整報告
報告附件：出席國際會議研究心得報告及發表論文
處理方式：本計畫可公開查詢

中　華　民　國 94 年 5 月 30 日

摘要

本計劃第二年期的成果以開發 OFDM 系統的基頻訊號處理演算法以及架構。特別著重於同部問題的解決因為它是 OFDM 系統效能高低的及重要關鍵。

有兩項主要成果。首先、我們分析並改進了一個用於符元(symbol)同步的演算法，這個演算法也是之前由我們為差分調變式 OFDM 系統所提出的。我們將其進一步簡化以適合低功率實現。第二、我們針對一個 OFDM 技術的實際應用、也就是所謂的多頻帶 OFDM 的超寬頻系統(MB-OFDM UWB)建立一套完整的同步策略。此系統是無線個人區域網路的可能技術選擇，低功率是必要條件，我們企圖以交換可接受的效能損失來達成適合低功率實現的低複雜度演算法。

Abstract

In the second year of our project, we continue developing the suitable algorithms and architectures of base-band signal processing for OFDM-based communication systems. The emphasis is especially on synchronization since it is a key issue of determining the performance of OFDM systems. There are two major accomplishments. First, we analyzed and furthered enhanced by reducing computation complexity a symbol synchronization algorithm previously proposed by us for differentially-modulated OFDM systems. Second, a comprehensive synchronization strategy for a specific application of OFDM technology, namely the Multi-Band OFDM Ultra-Wide Band (MB-OFDM UWB) system, is developed with the emphasis on low complexity algorithms.

關鍵詞

多輸入多輸出，球形解碼演算法，多樣化編碼

Keywords

OFDM, UWB, base-band signal processing, synchronization

目錄

1. Introduction

Our emphasis has been on developing the suitable algorithms and architectures of base-band signal processing for OFDM-based communication systems. Special attention has been paid to the synchronization issue, since it plays a key role in determining the performance of OFDM-based systems, and there is a lot of room to trade-off between performance and computation cost.

Two major accomplishments are discussed in this report. First, we analyzed and furthered enhanced by reducing computation complexity a symbol synchronization algorithm previously proposed by us for differentially-modulated OFDM systems. Second, a comprehensive synchronization strategy for a specific application of OFDM technology, namely the Multi-Band OFDM Ultra-Wide Band (MB-OFDM UWB) system, is developed. MB-OFDM UWB technology is a highly-possible candidate for the next-generation wireless personal area networks. Low power consumption is a must for such applications. Therefore, our development strategy is to sacrifice certain degree of performance in exchange for algorithms of very low complexity.

2. A Low-Complexity OFDM Symbol Timing Algorithm

In orthogonal frequency division multiplexing (OFDM) communication systems, data is modulated onto numerous sub-carriers. In wireless environment, the transmitter usually transmits OFDM symbols in a packet-based fashion. The transmission, however, will be distorted by the unknown characteristics of the channel. As a result, the received OFDM symbols in a packet may not be recognizable.

To mitigate the channel effects often a so-called circular prefix (CP) and/or suffix is introduced. These prefixes and/or suffixes are inserted between contiguous OFDM symbols and act as guardian intervals to reduce the possibility that waveforms interfere with each other.

At the receiver side, therefore, it is crucial to separate contiguous OFDM symbols, i.e., the boundaries of each OFDM symbols should be set such that no substantial “leakage” from neighboring OFDM symbols exists. The task of properly determining the start and end of each individual OFDM symbol and compensating any timing offset is called symbol timing synchronization, or symbol synchronization. Often a

training signal sequence is used to facilitate this task. Currently, using initial timing synchronization preamble is the most prevalent means in burst applications [1].

Most of the existing methods of symbol timing synchronization fall into two major categories. The first is based on signal processing in frequency domain. This type of method first calculates the fast Fourier transform (FFT) of the received signal and the phase angle of each tone. The differences between the phase angles of each tone and a set of pre-determined reference phase angles are calculated. Then the phase differences are processed by, for example, fitting to a linear regression model. In this case, the timing offset can be estimated from the slope of the regression line. The second category is based on signal processing in time domain. Usually the received signal is correlated with a pre-determined reference time-domain signal, such as in the methods based on ML [2], MMSE [3], or correlation [1] metrics.

Time domain methods often suffer significant performance degradation when strong co-channel interference or Gaussian noise is present. Properly designed frequency domain methods can achieve excellent performance. However, they often suffer from heavy computation required by processing the phase angles obtained from the FFT of received signals. Also, due to their reliance on sophisticated signal processing algorithms, often they are not robust enough under conditions of severe noise. In this report, a frequency domain method with low complexity for OFDM symbol timing synchronization is described.

Signal Model

The OFDM signal is generated at base-band by taking the inverse fast Fourier transform (IFFT) of quadrature phase shift keyed (QPSK) sub-symbols. The samples of the transmitted signal can be expressed as:

$$x(k) = \frac{1}{\sqrt{N}} \sum_{n=0}^{Nu-1} c_n \exp(j2\pi kn / N), -Ng \le k \le N-1$$

,

where c_n is the modulated data, N is the number of IFFT points, Nu is the number of sub-carriers, and Ng is the number of guard samples. Consider a channel with path gain $\{h_l : l = 0, 1,\ldots, k\text{-}1\}$ and the corresponding path delays $\{\tau_l\}$. We assume that the path delays are sample-spaced. Hence $\{h_l\}$ represents the discrete-time channel impulse response.

To simplify the illustration of the algorithm, we take the received samples after FFT module (Fig.1) as:

$R_{i,k} = a_{i,k} + b_{i,k} \cdot j = X_{i,k} \cdot H_{i,k} + N_{i,k},\ k = 1, \mathrm{K}\ , N,$

where k is a tone index, i is a received symbol index, $R_{i,k}$, is a received symbol for tone k, $a_{i,k}$ is the real part of $R_{i,k}$, $b_{i,k}$ is the imaginary part of $R_{i,k}$, $X_{i,k}$ is the transmitted symbol for tone k, $H_{i,k}$ is the channel attenuation for tone k, and $N_{i,k}$ is channel noise affecting tone k. That is, $R_{i,k}$ represents a point on the complex plane for tone k of the i-th received OFDM symbol.

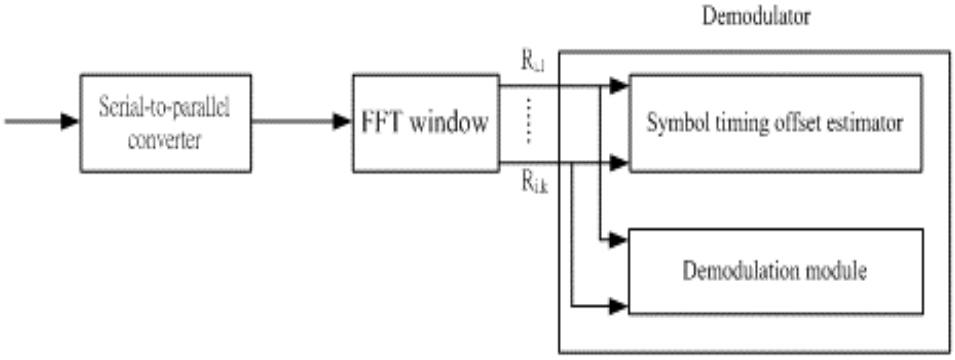

Figure 1

Differential Phase Offset

Before going to the details of the algorithm, the concept of differential phase offset (DPO) is introduced as a metric that contains information of any misalignment of symbol timing. In the following, for the sake of simplicity, noise is neglected and only a single time shift is considered. The pair of time domain signal $x(t)$ and its FFT X_k is represented as:

$x(t) \Leftrightarrow X_k = A_k \exp(j\phi_k)$.

The correspondence varies in the frequency domain as a phase rotation when a timing offset is introduced in time domain as given by:

$x(t-n) \Leftrightarrow \hat{X}_k = A_k \cdot \exp(j\phi_k) \cdot \exp(-j\frac{2\pi nk}{N}) = A_k \exp(j\Psi_k),$ where n is the timing offset and N is the symbol length. In the context of symbol timing estimation, A_k is the amplitude, ϕ_k is the correct phase angle when there is no symbol timing offset, and

Ψ_k is the phase angle when the symbol timing offset n exists. The task of symbol timing estimation is to determine the value of n in order to compensate for it and obtain correct phase angles.

Let the phase offset be the gap between received phase angle Ψ_k and the correct phase angle ϕ_k (Fig. 2), then DPO (denoted by Δ_k) is defined for the neighboring k-th and $(k+1)$-th tone as the difference, such that:

$\Delta_k = (\Psi_{k+1} - \phi_{k+1}) - (\Psi_k - \phi_k) = -\frac{2\pi(k+1)n}{N} + \frac{2\pi kn}{N} = -\frac{2\pi n}{N}$. Clearly, the information of symbol timing offset n is encoded in the DPO. Assuming there are K (indexed by k = 1 to K) sub-carriers in an OFDM symbol, then there will be $(k-1)$ DPOs (indexed by k = 1 to $K-1$) available for one OFDM symbol. From the definition of Δ_k, we know a delay/ahead in time domain will introduce a negative/positive phase in frequency domain. So, the range of Δ_k is from $-\pi$ to π. But for the simplicity of calculation, Δ_k maps to the new range of 0 to 2,.and the histogram will be done by simple comparisons.

The Symbol Timing Estimator

To summarize, the operation of the estimator is shown in figure 2. To estimate the symbol timing offset, a histogram of DPOs is first generated. Then, post-processing of the histogram provides an estimation of symbol timing offset. The position of the histogram peak is thought to indicate the value of $2\pi n/N$.

First, the gap between the phase angle and the correct phase of each tone is calculated, i.e., for each k, the difference $(\Psi_k - \phi_k)$ is calculated (Fig. 2). Note that since the calculation is done with mod 2钉 arithmetic, the result will be wrapped within the range of 0 to 2钉. Then, the DPO (denoted by Δ_k) is calculated for k = 1 to $K-1$. This calculation is also done with mod 2钉 arithmetic, and so the result is between 0 and 2钉. There are $(K-1)$ DPOs calculated for one OFDM symbol, but the

receiver is not restricted to use all of them for the purpose of symbol timing synchronization. A subset of the calculated DPOs may be used. Nor is the receiver restricted to use one OFDM symbol's worth of data to estimate the symbol timing offset. More than one OFDM symbol can be used if conditions permit. For example, if N OFDM symbols and $(K-1)$ DPOs per symbol are used, there will be $N(K-1)$ DPOs to be processed. In this paper, only the case of one symbol is described for the sake of simplicity. The case of multiple symbols is a straightforward generalization that can be done easily.

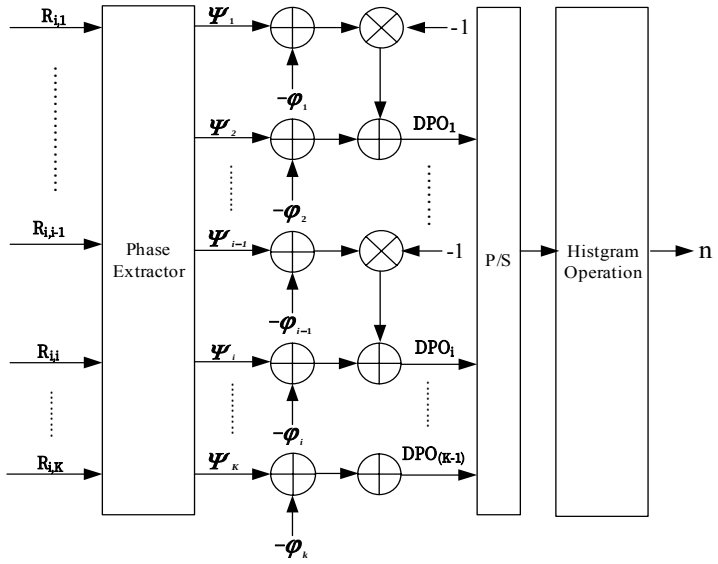

Figure 2

Next, the histogram of Δ_k is obtained. The interval from 0 to 2π is normalized to a new range from 0 to 2^N-1. And the interval from 0 to 2^N-1 is divided into 2^L bins. The key idea of the method is to fetch the first L bits of each normalized Δ_k to be the selector of a MUX and a DEMUX (Fig. 3). Each address of a register, which is used for saving the current value to a corresponding bin, is treated as the lower boundary of each bin. The value stored in each register will be fetched and add 1 to the value, then the new value will be returned to the same register when a register is selected by a truncating Δ_k. After all Δ_k are checked, the histogram operation is done at the same time. The histogram of Δ_k is further processed to determine the timing offset n. The peak of histogram, i.e., the bin which has the highest number, is chosen. Assume the peak occurs at the *l*-th bin. The *l*-th bin from $(l-1)2\pi/L$ to $l2\pi/L$ represents

the possible values for n from $(\frac{l-1}{L})N$ to $(\frac{l}{L})N$. Therefore, the estimation of n can be chosen as $(\frac{l-0.5}{L})N$, i.e., the average of the possible values. Note the estimation of n will be $(\frac{l-0.5}{L}-1)N$ if the lower boundary of the *l*-th bin is greater than 钉. The reason why $(\frac{l-0.5}{L})$ minuses 1 comes form the phase need to be wrapped between $-\pi$ to π. Once the symbol timing offset is estimated, the symbol timing synchronization can be easily achieved by adjusting the boundaries of each time domain OFDM symbol. A positive n means that the current boundaries are behind the correct boundaries and need to be moved ahead by n samples. A negative n means the boundaries need to be delayed by n samples.

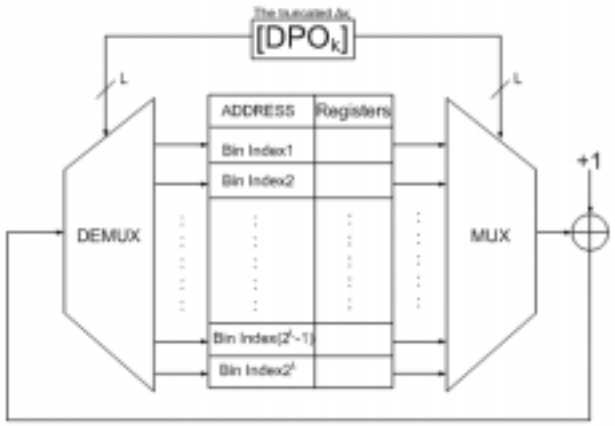

Figure 3

Performance

Simulations have been conducted to evaluate the performance of the algorithm. The OFDM system parameters used are 128 subcarriers, 128 point IFFT/FFT, a cyclic prefix of 32 samples and a guard interval of 5 samples [5]. The value of a subcarrier frequency spacing is 4.125MHz (=528MHz/128) and a symbol time is 312.5ns. The subcarrier modulation is QPSK and all channels are set to be 16 taps. The channel is modeled as Rayleigh fading. A channel is static in each simulation but changes from one simulation to another. The object of the symbol timing synchronization is to give a proper timing estimate to maintain the orthogonality among subcarriers. For this reason, the timing estimate should be in the ISI-free part of the cyclic prefix. Fig. 4 shows the results obtained from 100 Monte Carlo trials at SNR = 10dB [1] by using correlation method (S&C) and the proposed method with 16, 32, 64, and 128 bins. The figure shows that the performance of proposed method has better results without

the need of any ad hoc time shift.

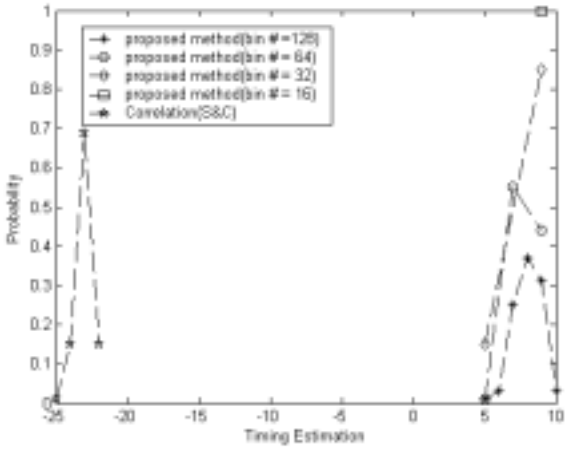

Figure 4

3. MB-OFDM UWB Systems

By the FCC's (U.S. Federal Communications Commission) definition, UWB communication systems use signals with -10dB fractional bandwidth that is larger than 20% of the center frequency, or greater than 500 MHz. Besides, FCC gives the rigid spectrum mask which the power spectrum density of the UWB signal should be within. With the low power spectrum density of UWB systems, the UWB signals could be viewed as noise by other narrow-band devices. On the other hand, for UWB systems with a wide PSD, the disturbance from narrow-band systems occupies merely a small fraction of its bandwidth; therefore, the data carried by UWB signal can be easily recovered with FEC.

Synchronization is an essential task for any digital communication system. Without effective synchronization algorithms, it is not possible to reliably receive the transmitted data. From the digital base-band algorithm design engineer's perspective, synchronization algorithms impose a major design problem that has to be solved to build a successful product.

OFDM can be used in the context of continuous mode and packet-mode transmission networks. The two transmission schemes require somewhat different approaches to the synchronization problem. Continuous-mode systems transmit data continuously, so a typical receiver can initially spend a relatively long time to acquire the signal and then switch to tracking mode. On the other hand, the synchronization has to be acquired within a very short time after the start of the packet to archive high

data rates for packet-mode systems.

In MB-OFDM UWB systems, the transmitted signals are OFDM symbols carried by a sequence of carrier frequencies depending on the TFC. Beside the usual OFDM synchronization tasks including packet detection, carrier frequency synchronization, and timing recovery, the MB-OFDM UWB system also needs the band alignment procedure which aligns the transmitter time-frequency sequences.

Signal Detection

In MB-OFDM UWB systems, there are 30 preambles as training sequences to train the receiver, as mentioned in 2.2. The four patterns for each channel have low cross correlation property to each other. And for each of the preamble, the autocorrelation with time shift is almost equal to zero. Just like the direct sequence spread spectrum, the preamble can be used to channelize piconets. So the proposed signal detection scheme is a match filter (MF), as shown in figure 5. For the simplicity of implement, the match filter coefficients are the signs of the preamble, there for there will be no multiplier in the match filter. The MF is proposed to match the preamble pattern corresponding to the channel which the receiver is going to access. The match filter output is compare to a threshold to determine if the signal comes. For power saving purpose, a constant threshold is preferred in the system. If a proper threshold is setting, the signal detection will be robust to interference and noise.

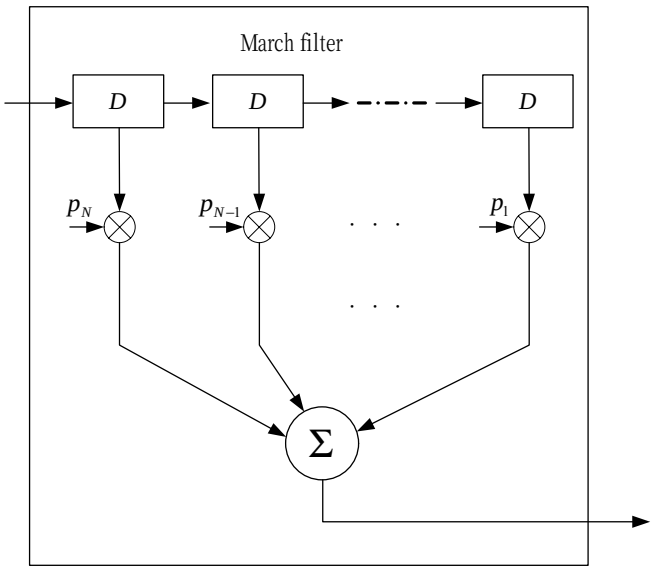

$p_i = \pm 1$ depending on the channel

Figure 5

Interferences

When there are two or more piconets operating at the same time, collision will happen in some band. Unfortunately, sometimes the power of interference is stronger than the desired signal. To simplify the detection algorithm, the MF collects the signal of one band, and there will be a probability of 1/3 that the MF output is interfered by the signal of other piconet. The signal detection algorithm must be designed robustly to the interference.

First of all, the interference should be modeled in mathematical form to formulate the statistic property of MF output. Take a look at the OFDM symbol, $s(t) = \sum_{n=-N/2}^{N/2-1} a_n e^{j2\pi n f_0 t}$, which can be represented as $s(t) = \sum_{n=-N/2}^{N/2-1} a_n w_n$, a weighting sum of modulated data. If the data are taken as random variables and N is large, s(t) is a Gaussian process based on the central limit theorem (CLT).

The OFDM symbol of MB-OFDM systems is composed of 128 tones and each tone carries a QPSK symbol of power equal to unity and tones of indexes {0 64 65 66 67 68} are null tones. The autocorrelation function is approximately equal to delta function, which means the approximate Gaussian process is also near to white. Therefore, the OFDM signal can be modeled as white Gaussian noise with zero mean because the DC tone is null. It will simplify the analysis of the MF output statistic property while the interference can be modeled as white Gaussian.

Simulation Platforms

There are two kinds of simulation platforms; one is take the SOP interference as white noise and pass through a multipath channel then add to the received signal. In the second kind model, the received signal is the desired signal incorporated with thermal noise and the signal generated from another piconet. As shown in figure 6.

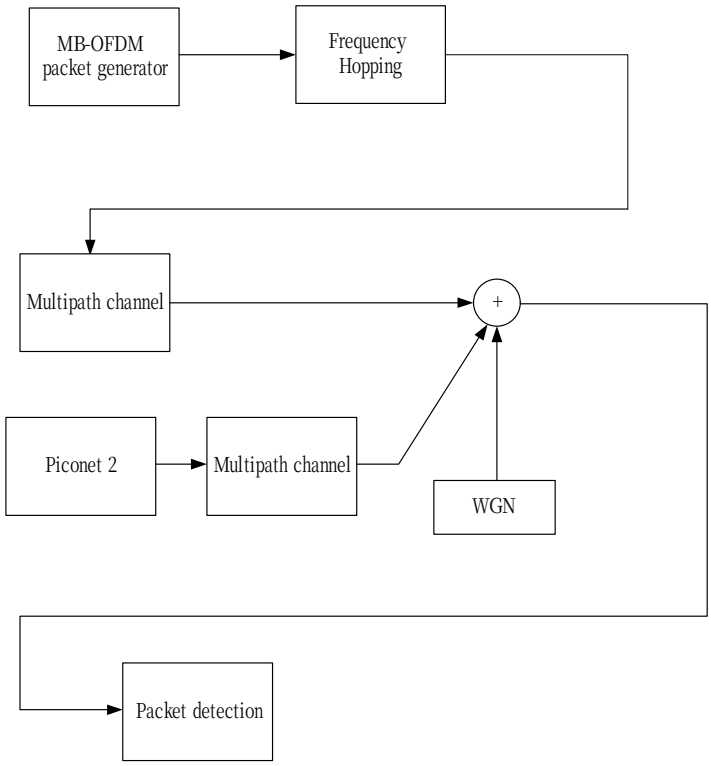

Figure 6

Threshold Settings

The threshold level is an import parameter of the detection algorithm. A simple setting method based on AWGN channel is derivate.

The received signal after sampling is $r_i = s_i + n_i$, where s_i is the transmitted signal and n_i is the noise and interference with distribution, $n_i \sim N(0,\sigma)$.

The output of the match filter is $m_i = \sum_{k=i-N+1}^{i} p_k s_k + \sum_{k=i-N+1}^{i} p_k n_k$

Let $\sum_{k=i-N+1}^{i} p_k s_k = A_i$, $\sum_{k=i-N+1}^{i} p_k n_k = w_i$, so

$$m_i = A_i + w_i$$

The value of A_i depends on the cross-correlation of the symbol and pattern, it is

reasonable to assume A_i equal to 0 if it is not the desired signal sequence. And w_i is a random variable with distribution $N(0,\sigma_v^2)$, where $\sigma_v^2 = N\sigma$. So defined two hypotheses, H_0 and H_1, where

H_0 : $m_i = w_i$

H_1 : $m_i = A + w_i$

Based on the proposal of MB-OFDM system, the value of A_i is 1300 when the received signal matches the pattern. So the value of m_i is a random variable of Gaussian distribution with variance $N\sigma^2$ and bias 0 or 1300 depending on the excess of boundary. The threshold can be set according to the desired false alarm rate or missing rate, as shown in figure 7. In figure 7, the SNR is -10 dB, and

$\sigma^2 = N \times 10^{-SNR/10}, N\sigma^2 = N^2 \times 10^{-SNR/10} = 163840$

$\sigma_v = \sqrt{N\sigma^2} = 404.77$

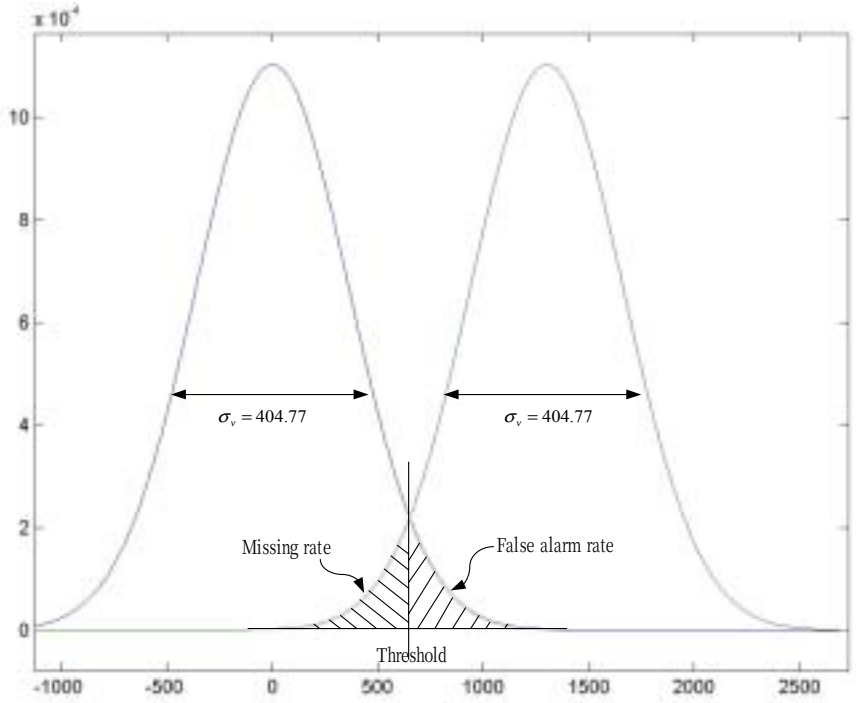

Figure 7

Due to the co-band interference of SOP, the SINR might get negative value in dB which means the power of interference is stronger than that of desired signal. The packet detection algorithm in MB-OFDM systems should be robust to this kind of

interference. It is important to how much noise the algorithm can tolerate. A plot of the missing rate versus SNR is shown in figure 8. As shown in this figure, the false alarm rate and missing rate is greatly increasing when SNR lower than -3dB. It is desired to design another algorithm more robust.

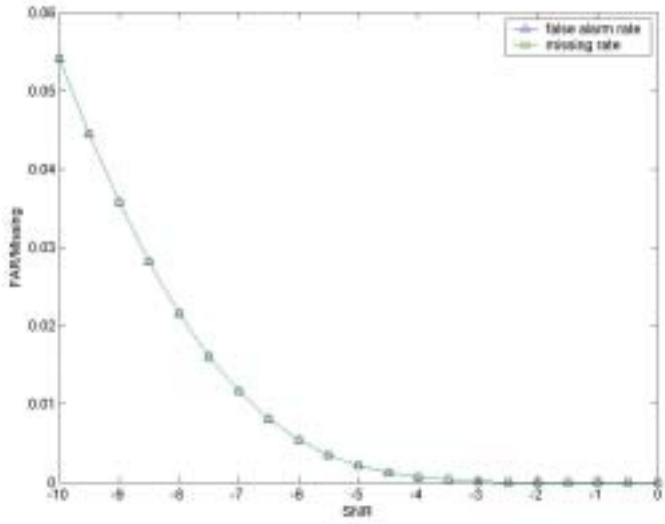

Figure 8

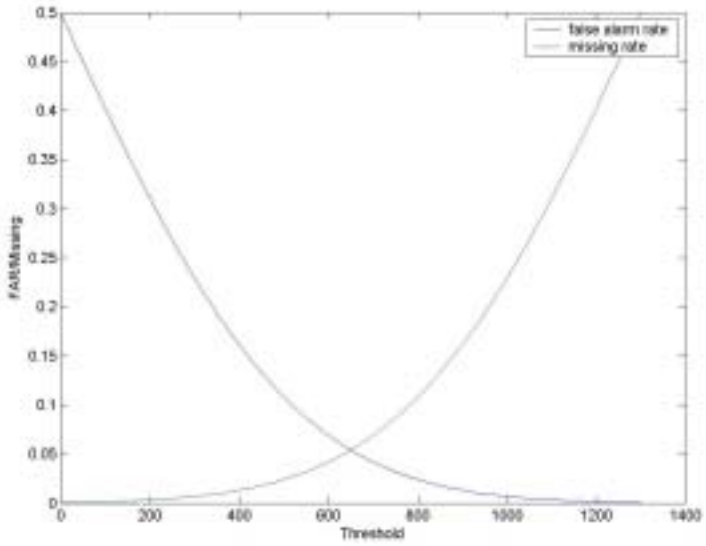

Figure 9

4. An Improved Signal Detector for MB-OFDM UWB Systems

In an MB-OFDM packet, there are 24 preambles defined in time domain for packet detection. The 24 preambles use the same pattern with a polarity. So there are 8 periodic training symbols in each band. If an auto-correlator with a period of delay is used, it is supposed that the performance will be better. The scheme is as shown in figure 10. The match filter output is multiplied with the previous output, it is desired to separate the mean value of the two hypotheses.

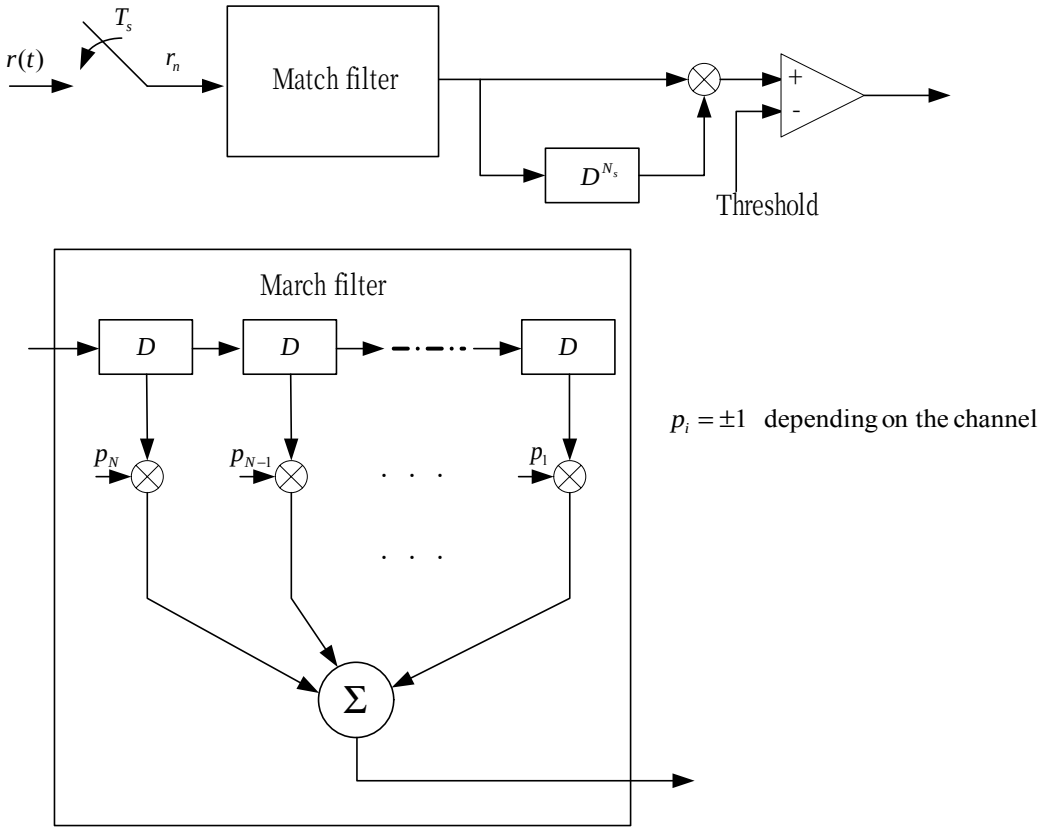

Figure 10

The delay correlator output is

$$\begin{aligned} d_i &= m_i m_{i-N_s} \\ &= (A_i + w_i)(A_{i-N_s} + w_{i-N_s}) \\ &= A_i A_{i-N_s} + A_i w_{i-N_s} + A_{i-N_s} w_i + w_i w_{i-N_s} \end{aligned}$$

The two hypotheses can be formulated as

H_0 : $d_i = w_i w_{i-N}$

H_1 : $d_i = A^2 + A(w_{i-N_s} + w_i) + w_i w_{i-N_s}$

The distribution of hypothesis 0 is the product of two Gaussian variable with mean equal to zero. So the PDF is

$$f(d_i) = \frac{1}{\pi\sigma^2} K_0\left(\frac{|d_i|}{\sigma^2}\right),$$

where $K_0(x)$ is the modified Bessel function of second kind.

But for H_1, the PDF of d_i has no close form. It can be expressed in the form of a double infinite series in Whittaker function. But this form is too complex to use it practically. A simpler one in integration form is derived.

$$\begin{aligned} F_Z(z) &= P[Z < z] \\ &= \int_0^\infty f_Y(y)\int_{-\infty}^{z/y} f_X(x)dxdy + \int_{-\infty}^0 f_Y(y)\int_{z/y}^\infty f_X(x)dxdy \\ &= \int_0^\infty f_Y(y)\left(1 - Q\left(\frac{z/y - A}{\sigma}\right)\right)dy + \int_{-\infty}^0 f_Y(y)Q\left(\frac{z/y - A}{\sigma}\right)dy \\ &= Q\left(\frac{-A}{\sigma}\right) - \int_0^\infty f_Y(y)Q\left(\frac{z/y - A}{\sigma}\right)dy + \int_{-\infty}^0 f_Y(y)Q\left(\frac{z/y - A}{\sigma}\right)dy \end{aligned}.$$

where $f_Y(y) = \frac{1}{\sqrt{2\pi\sigma}}\exp\left(\frac{(y-A)^2}{2\sigma^2}\right)$ $f_X(x) = \frac{1}{\sqrt{2\pi\sigma}}\exp\left(\frac{(x-A)^2}{2\sigma^2}\right)$

$$Q(x) = \frac{1}{\sqrt{2\pi}}\int_x^\infty e^{t^2/2}dt$$

Then the PDF of Z is

$$f_Z(z) = \frac{d}{dz}P[Z < z] = -\frac{d}{dz}\int_0^\infty f_Y(y)Q\left(\frac{z/y - A}{\sigma}\right)dy + \frac{d}{dz}\int_{-\infty}^0 f_Y(y)Q\left(\frac{z/y - A}{\sigma}\right)dy.$$

Although the final term is integration from 0 to infinite, but it is shown that the Q(x) converges to zero very fast. So it is easier to use numerical method to approximate PDF and CDF. The PDF and CDF is as shown in figure 11 figure 12. The CDF plot is more useful for determining the missing rate. When a threshold is set, the corresponding CDF value is the missing rate. Also, the CDF of H_0 hypothesis is used to determine the false alarm rate. The corresponding false alarm rate is 1 minus the CDF value of the threshold. The two curves are shown in figure 13.

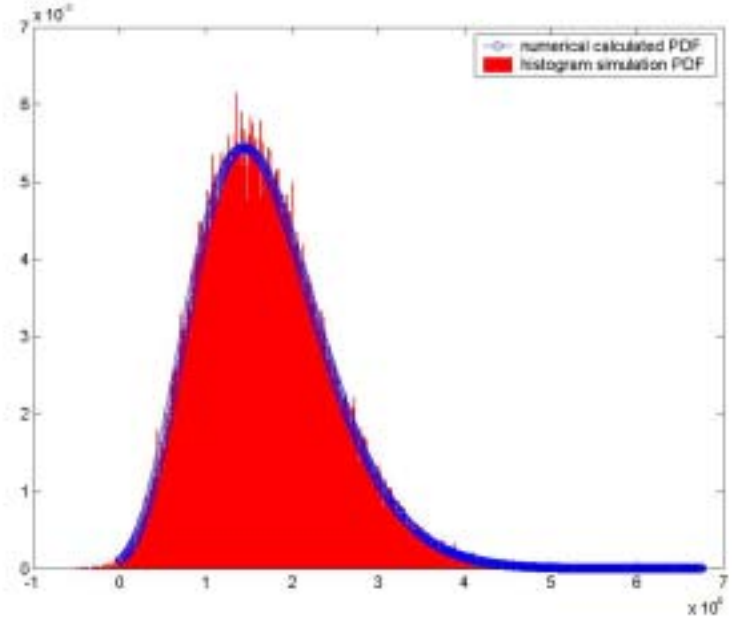

Figure 11

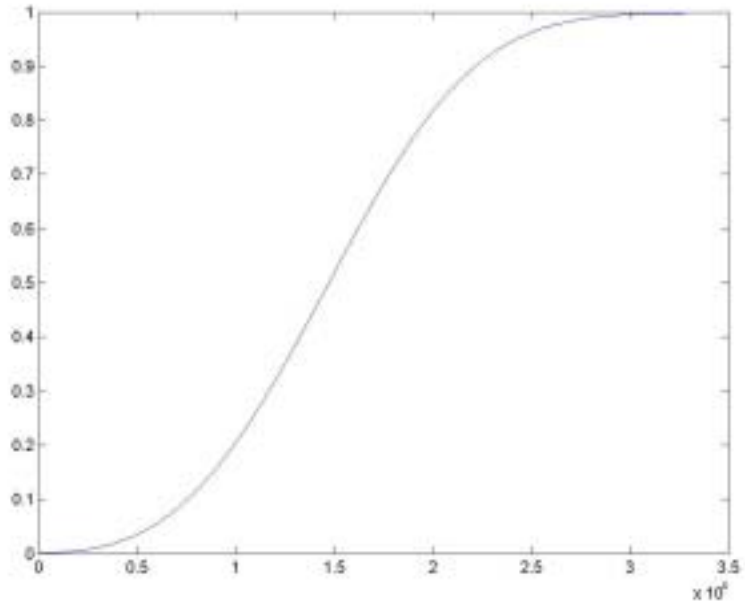

Figure 12

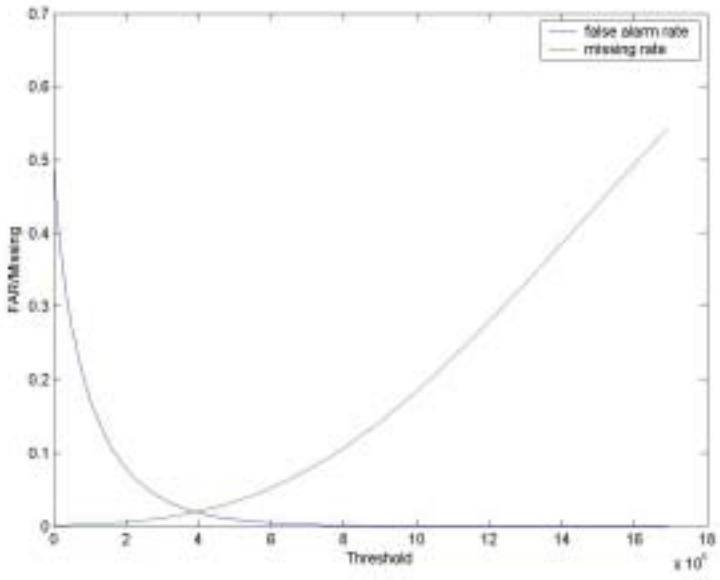

Figure 12

It is important to check the robustness of the algorithm. First of all, the algorithm should be anti-interference. When threshold is set at the value which has equal false alarm rate and missing rate, the relative variant of the FAR and missing rate is as shown in figure 14.

Besides the interference, the carrier frequency offset (CFO) of the algorithm should be considered. The effect of CFO under AWGN channel in base-band is

$$r_i = s_i e^{j\Delta fiT} + n_i$$ where r_i : the ith sample of the received signal
s_i : the ith sample of the transmitted signal
Δf : carrier frequency offset
T : sampling time

The match filter output is then affected by the CFO. The value of A then becomes

$$A = \sum_{i=0}^{N-1} p_i s_i e^{j2\pi\Delta fiT}$$

There exists performance degradation for the value of A. However based on the MB-OFDM proposal, the transmitter and receiver oscillator frequency offset is in $\pm$ 20 ppm, so the CFO between transmitter and receiver is $\pm$40 ppm in worst case. Assume maximum carrier frequency is 10 GHz, and then the maximum CFO is 400

KHz. The maximum degradation happens in ±400 KHz, and the corresponding degradation is -0.1307 dB. The value is small enough to neglect the effect.

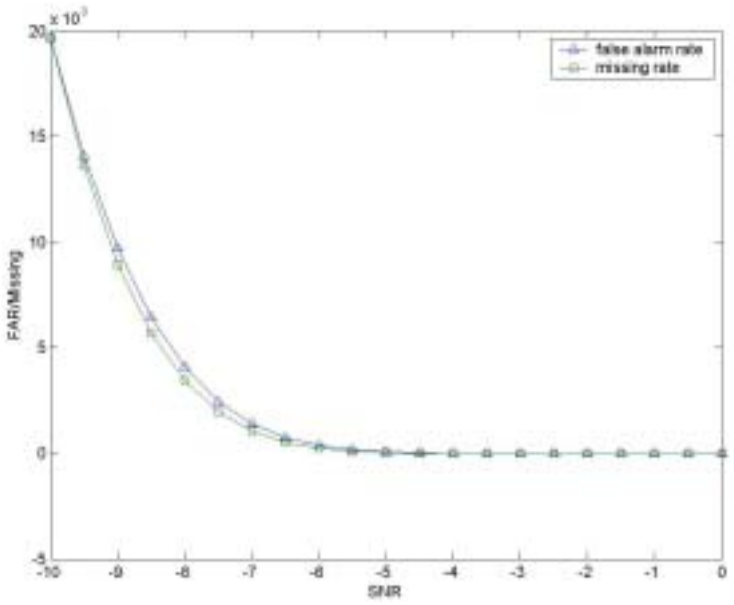

Figure 14

5. Other Synchronization Issues

Carrier Frequency Offset and Sampling Timing Offset

An OFDM symbol is a linear combination of orthogonal harmonic functions with a truncated window function. Assume a rectangular window function is used, then the frequency domain representation of an OFDM symbol is shown is figure 15. The sampling in frequency domain should be in the peaks of the sinc functions which results in no ICI. But if the transmitter and receiver oscillators mismatch, the sampling in frequency domain will not in the peaks, so the ICI occurs and the desired signal degrades, as shown in figure 15.

The effect caused by CFO is the SNR degradation, and the degradation can be represented as

$$D \approx \frac{10}{3\ln 10}(\pi \Delta f T)^2 \frac{E_s}{N_0}.$$

In MB-OFDM system, the maximum CFO is ±40ppm. For 10 GHz carrier frequency, the CFO is ±400 KHz which is the worst case. The degradation of the

SNR versus E_s/N_0 is then plotted as figure 16. As shown in this figure, the SNR degradation is very small compared to E_s/N_0. So the ICI caused by CFO in MB-OFDM system can be neglected.

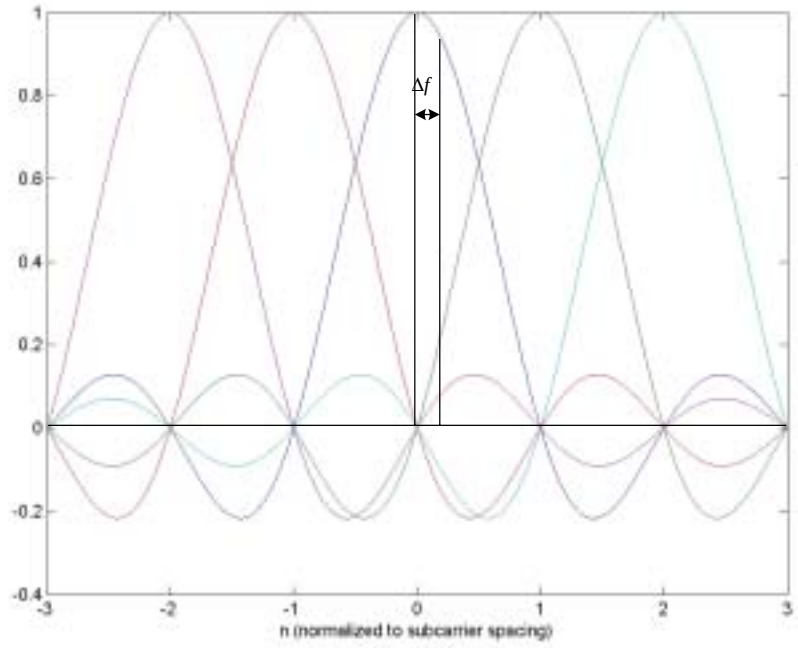

Figure 15

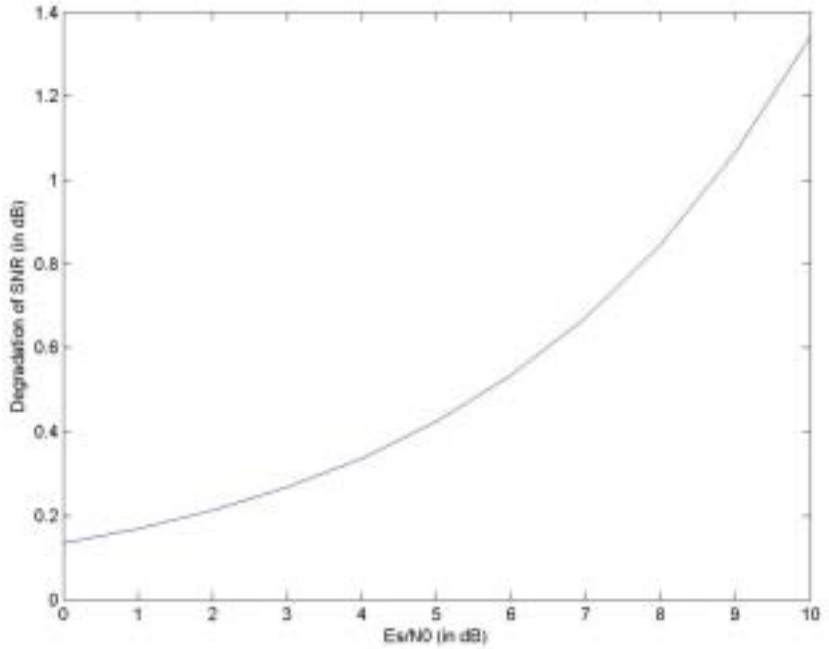

Figure 16

Besides ICI, the CFO rotates the mth OFDM symbol with angle $2\pi(m\Delta fT_s + T_g)$,

and each subcarrier of the OFDM symbol suffers this phasor. So the receiver should compensate this phase.

Timing recovery could be further divided into symbol synchronization and sampling clock synchronization. The purpose of symbol synchronization is to find the correct position of the fast Fourier transform window.

The sampling clock offset causes three effects: FFT window drift, ICI, and symbol rotation [6].

Let $\xi = \frac{T' - T}{T}$ where T' = receiver sampling time

T = transmitter sampling time .

The drift at mth OFDM symbol caused by sampling clock offset is:

$$FFT \text{ window drift} = \frac{1}{T}\left[(mN_s + N_g)T' - (mN_s + N_g)T\right]$$
$$= (mN_s + N_g)\xi$$

where N_s : sampling points per OFDM symbol

N_g : guard interval .

The FFT window drift effect is as shown in figure 17.

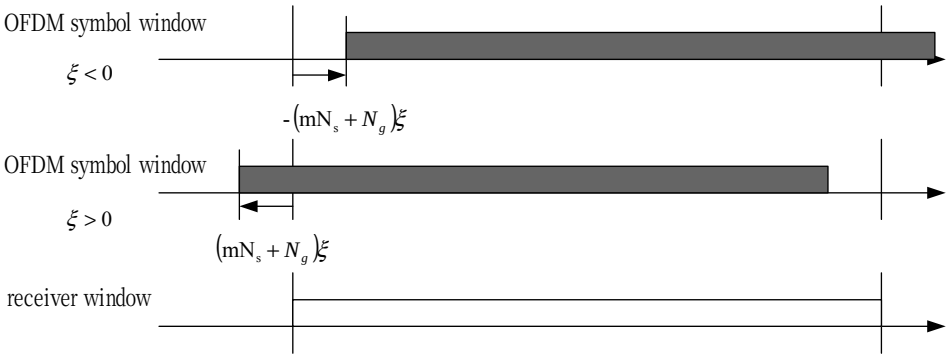

Figure 17

With only FFT window drift effect considered, the demodulated data will have $2\pi \frac{n(mN_s + N_g)}{N}\xi$ phase rotation. Now define $\tilde{a}_m^n = a_m^n e^{j2\pi \frac{n(mN_s+N_g)}{N}\xi}$.

The demodulated n-th symbol of the m-th OFDM symbol with sampling frequency f_s and sampling frequency offset Δf is

$$R_m^n = \tilde{a}_m^n I_{n,n} + \sum_{\substack{k=0 \\ k\neq n}}^{N-1} \tilde{a}_m^k I_{k,n}$$

$$where\ \ I_{k,n} = \frac{1}{N} \frac{\sin(\pi(k(1+\xi)-n))}{\sin\left(\frac{\pi}{N}(k(1+\xi)-n)\right)} \exp\left(j\pi \frac{N-1}{N}(k(1+\xi)-n)\right)$$

.

The SNR degradation due to sampling frequency offset is [7]:

$$D_n \approx 10\log_{10}\left(1 + K_n \frac{E_s}{N_0}\left(\frac{\Delta f_s}{f_s}\right)^2\right)$$

$$\text{where } K_n = \frac{1}{N^2} \sum_{\substack{k=0 \\ k\neq n}}^{N-1} \frac{\pi^2 k^2}{\sin^2\left(\frac{\pi}{N}(k-n)\right)}$$

.

Now, to evaluate the degradation effect of sampling clock offset. As log function is a monotonic increasing function, the maximum SNR degradation happens at the tone of maximum K_n. For MB-OFDM system, the tone index and K_n relationship is shown in figure 18, and the maximum value of K_n happens at the tone of index 123. Usually the sampling clock is generated from the same oscillator as carrier frequency oscillator. So the sampling clock offset is $\pm$40 ppm. With this K_n, the SNR degradation due to sampling clock offset is shown in figure 18. The degradation is minor to E_s/N_0.

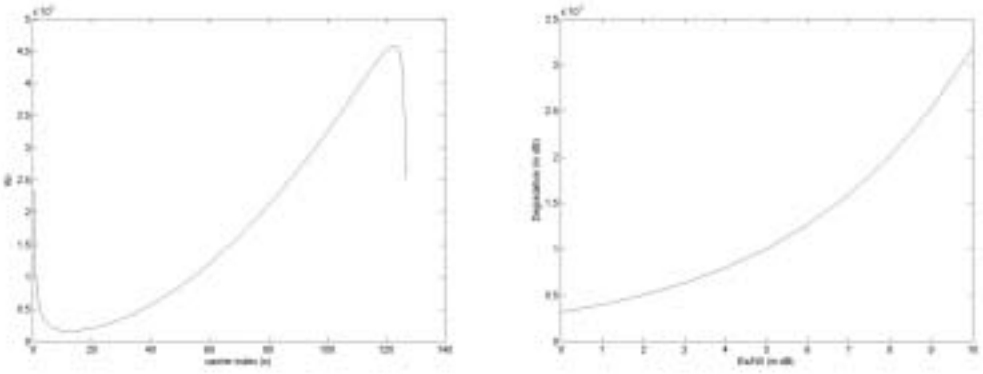

Figure 18

The phase rotation of nth tone of mth OFDM symbol can be concluded as:

$$\theta_m^n = 2\pi \frac{n(mN_s + N_g)}{N}\xi + \arg[I_{n,n}]$$
$$= 2\pi \frac{n(mN_s + N_g)}{N}\xi + n\pi \frac{N-1}{N}\xi$$
$$= n\left(2\pi \frac{mN_s + N_g}{N}\xi + \pi \frac{N-1}{N}\xi\right)$$
$$= n\kappa$$

where $\kappa = 2\pi \frac{mN_s + N_g}{N}\xi + \pi \frac{N-1}{N}\xi$.

The phase rotation is proportional to the tone index, as shown in figure 19.

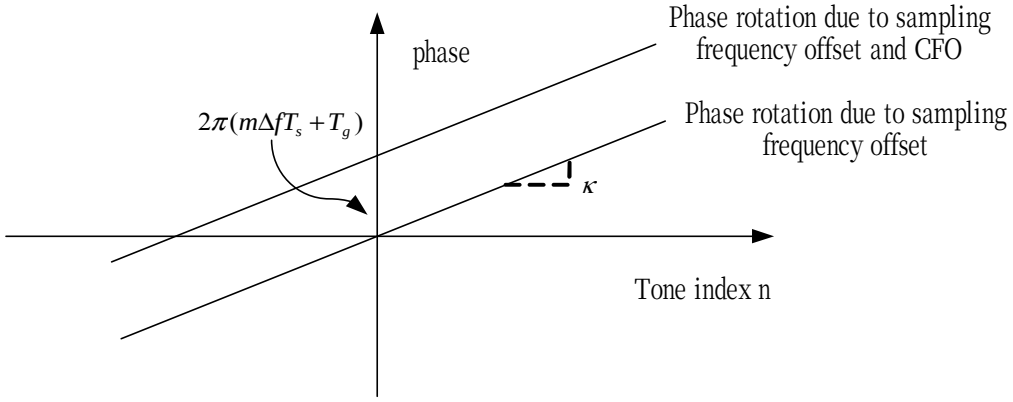

Figure 19

6. A Synchronization Strategy for MB-OFDM UWB Systems

From the above discussion, since ICI caused by CFO and sampling clock offset in MB-OFDM play minor role in performance, the synchronization issue becomes how to rotate the phase back and keep tracking the timing phase.

The synchronization flowchart is as shown in figure 20. During signal detection, the initial symbol timing is done at the same time. The channel estimation makes use of the CE portion of the preamble. In every OFDM symbol, 12 pilot tones are inserted. The 12 pilot tones can be used for tracking the phases. As knowing the phase rotation, the receiver should compensate the phase back and then demodulate the data. And the

phase rotation caused by the timing phase offset should be compensated for the right next OFDM symbol.

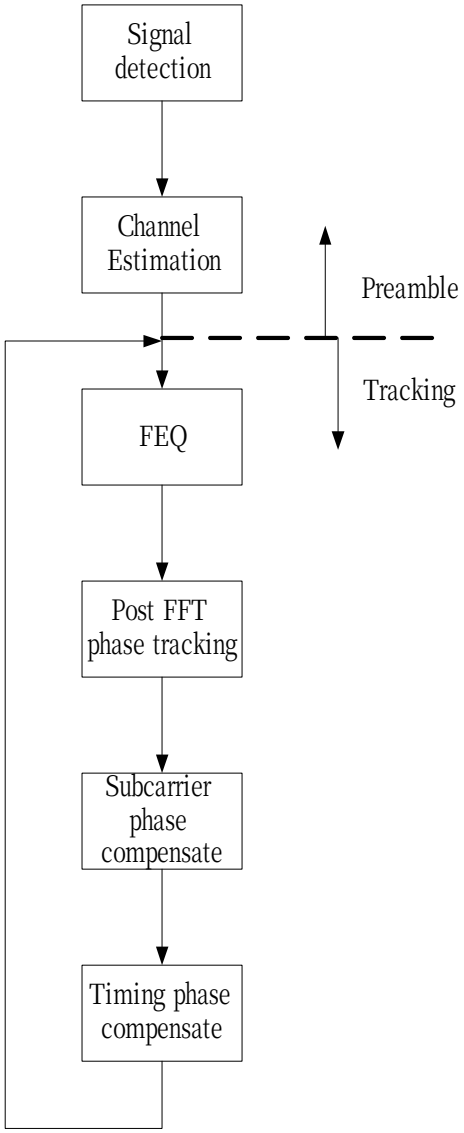

Figure 20

Because there is no frequency and phase compensation mechanism, the estimated channel incorporates the some phase rotation due to CFO and sampling clock at the CE symbol, and the rotation will be compensated by the frequency domain equalizer.

Because MB-OFDM is used in home or office environment and operated in high data rate, it is reasonable to assume the channel impulse response is the same during the whole packet. The most common channel estimation makes use of frequency domain approach.

The received signal in frequency domain is

$$R_m^n = H_n a_m^n + W_m^n,$$

and the estimated channel is

$$\hat{H}_n = R_m^n a_m^{n\,*} / \left|a_m^n\right|^2 = H_n + W_m^n a_m^{n\,*} / \left|a_m^n\right|^2 \quad ,$$

where $\left|a_m^n\right| = 1$ for MB-OFDM system, so

$$\hat{\mathrm{H}}_\mathrm{n} = \mathrm{R}_\mathrm{m}^\mathrm{n} \mathrm{a}_\mathrm{m}^{\mathrm{n}\,*} = \mathrm{H}_\mathrm{n} + \mathrm{N}_\mathrm{m}^\mathrm{n} \quad \text{where } \mathrm{N}_\mathrm{m}^\mathrm{n} = W_m^n a_m^{n\,*} \quad .$$

The phase rotation due to CFO and sampling clock offset are parallel shift and linear increasing with the tone index. And the pilot position is symmetry about DC tone. So in the tracking loop, the common phase term is the average of the pilot tone phase rotation. And the slope of the phase line can be used to estimate the sampling phase (e.g. average the slope of each adjacent pilot pair). And then the phase rotation of each sucarrier can be calculated. That is

$$\kappa = \frac{1}{N_p} \sum_{\mathrm{n} \in \text{pilot tone}} \arg(R_m^n) - \arg(p_m^n) - \theta_c \quad .$$

In the above equation, the minus of common phase term is necessary. Because the arctan function has an ambiguity of 2π period. To prevent from the ambiguity, there should not be parallel shift and the slope of the phase increment should not be too large. The parallel shift is canceled by compensating the common phase term. To prevent the occurrence of large slopes, the sampling phase offset should be compensated frequently enough.

Recall that the slope of the phase increment is $2\pi \frac{mN_s + N_g}{N} \xi + \pi \frac{N-1}{N} \xi$. The term $2\pi \frac{N_g}{N} \xi + \pi \frac{N-1}{N} \xi$ is compensated by the FEQ, and the remaining term $2\pi \frac{mN_s}{N} \xi$ which results from the effective FFT window drift due to sampling clock offset. According to this slope, the range of phase rotation in an OFDM symbol is $2\pi m N_s \xi$. It means the sampling phase drift should be contained within one sample. If the sampling clock offset is a constant value, the slope tends to increase or decrease symbol by symbol depending on the sign of ξ. So when the slope of the phase rotation slope is greater than π/N, it means the FFT window is late for about half a sample and the FFT window should move forward one sample. When the slope is less than -π/N, it means the FFT window is about early for half a sample and the FFT window

should move backward one sample. The simulation shows that this coarse compensation method is good enough for MB-OFDM UWB systems, at the same time a low-complexity receiver remains possible.

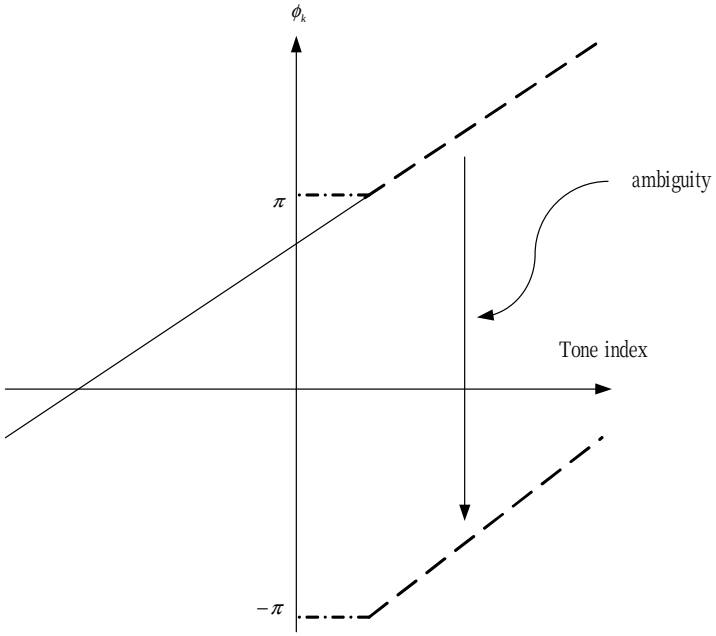

Figure 21

7. 計劃成果自評

我們在兩方面的研究成果較為突出。第一是我們分析並改進了一個用於符元(symbol)同步的演算法，這個演算法也是之前由我們為差分調變式 OFDM 系統所提出的。我們將其進一步簡化以適合低功率實現。此項成果已投至國際會議[8]即將發表。第二、我們針對一個 OFDM 技術的實際應用、也就是所謂的多頻帶 OFDM 的超寬頻系統(MB-OFDM UWB)建立一套完整的同步策略。此系統是無線個人區域網路的可能技術選擇，低功率是必要條件，我們企圖以交換可接受的效能損失來達成適合低功率實現的低複雜度演算法。由於 OFDM 是一個成熟的技術，基頻訊號處理演算法以及架構方面的研究已漸趨完備，然而在同步問題上、特別是針對 UWB 的應用上、仍有發揮的空間，我們預期將第二項成果加以擴充成期刊論文。

8. References

[1] T.M. Schmidl, D.C. Cox, “Robust frequency and timing synchronization for OFDM,” Communications, IEEE Transactions on, Volume: 45 Issue: 12, Dec. 1997, Page(s): 1613-1621M

[2] Jan-Japp Van de Beek, Magnus Sandell, Per Ola BOrjesson, “ML Estimation of Time and Frequency Offset in OFDM Systems,” IEEE Transactions on Signal Processing, in press

[3] Hlaing Minn, Vijay K. Bhargava, Khaled Ben Letaief, “A Robust Timing and Frequency Synchronization for OFDM Systems,” IEEE Transactions on Wireless Communications, Volume: 2 No. 4 July 2003, Page: 822-839.

[4] Jian Sun, Haitham M. A. Issa, Peiliang Qiu, “Frequency and Timing Synchronization and channel Estimation in Preamble Based OFDM System,.

[5]Anuj Batra et al, “Multi-band OFDM physical Layer Proposal for IEEE 802.15 Task Group 3a” IEEE P802.15-03/268r1 September, 2003, Page:1-69

[6] Pollet, T., M. van Bladel and M. Moeneclaey, “[0]BER Sensitivity of OFDM Systems to Carrier Frequency Offset and Wiener Phase Noise” IEEE Trans. on Comm. Vol.43 No.2/3/4, pp 191-193, Feb.-Apr. 1995

[7] Thierry Pollet, Paul Spruyt, and Marc Moeneclaey, “The BER Performance using non-synchronized sampling” Proc. of GLOBECOM, pp253-257, 1994

[8] Tzu-Hsien Sang, Sheng-Yi Hsu, and Tsung-Liang Chen, “A New Data-Aided OFDM Symbol Timing Synchronization Algorithm Based on Histogram Processing,” accepted for *the 2005 International Conference on Wireless Networks* (ICWN'05: June 27-30, 2005, Las Vegas, USA)